PULSE LASER RADIATION TRANSFER: MONTE CARLO SIMULATION AND COMPARISON WITH EXPERIMENT

Zhixiong Guo[*], Janice Aber[**], Bruce Garetz[**] and Sunil Kumar[*]
Polytechnic University, 6 Metrotech Center, Brooklyn, NY, USA
[*] Department of Mechanical, Aerospace and Manufacturing Engineering
[**] Department of Chemical Engineering and Chemistry

ABSTRACT. A three-dimensional Monte Carlo simulation of transient radiative transfer is performed for short pulse laser transport in scattering and absorbing medium. Experimental results of a 60 ps pulse laser transmission in scattering medium are presented and compared with simulation. Good agreement between the Monte Carlo simulation and experimental measurement is found. The refractive index of the scattering particles is found to influence strongly the prediction of transmitted pulse shape. Scaled isotropic scattering modeling is shown to be not sufficient in transient radiative transfer.

INTRODUCTION

The study of pulsed laser radiation transfer in strongly scattering medium has received increasing attention during the past few years, partly as a result of its wide applications to medical diagnosis and thermal therapy [1,2], remote sensing [3], and laser material processing of microstructures [1,4]. With the laser pulse width in the picosecond to femtosecond range, the time-dependence of radiative transport must be incorporated and transient radiation transfer formulated for such kinds of systems is salient.

The propagation of light in optically dense random media is characterized by multiple scattering, so that the diffusion approximation was often used to describe the transient radiation transport [5]. However, recent studies have demonstrated that the diffusion approximation fails to fully describe the backscattering light, because such light is compromised of a significant contribution of multiply scattered modes whose path lengths are comparable to the transport mean free path [6]. It also failed to describe transmitted light in some other experimental studies [7]. Very few studies have addressed transient radiative transfer by considering the fully transient radiative transfer equation. Kumar and Mitra [8] and Kumar *et al*. [9] are among the first to consider the entire transient radiative equation by using a variety of models for short-pulse applications. Previously, transient radiative transfer equation with a source of constant strength at the boundaries using Laplace transform and adding-doubling methods had been solved by Rackmil and Buckius [10]. Recently, Mitra *et al.* [11] solved wave-like transient radiative transfer equation using the P_1 approximation for a boundary-driven two-dimensional problem. Guo and Kumar [12] evaluated the scaled isotropic scattering results with the anisotropic scattering in transient radiative transfer. Tan and Hsu [13] developed integral equation formulation for transient radiative transfer.

Monte Carlo (MC) methods have been used extensively in steady-state simulations of radiative heat transfer [14]. Many researchers have also used the MC method to address transient laser-tissue interactions [15, 16]. However, an instantaneous, isotropic and point source was generally used to simulate the incident laser beam, and the system was generally restricted in one-dimensional slab.

Recently, Guo et al. [17] studied the characteristics of multi-dimensional transient radiative transfer using the MC method. They found that the MC method is very suitable for the study of pulse laser radiation transport in highly scattering medium because of its feasibility in handling the realistic physical conditions and the relatively inexpensive computation cost since only the incident laser photons are to be traced, even though the MC method is subject to statistical errors.

In the present study, a Monte Carlo approach is developed to simulate transient radiative transport of short pulse laser incident upon three-dimensional highly scattering media. The realistic physical models, such as the temporal and spatial Gaussian distributions of the laser beam, the Fresnel reflection at the media/air boundaries, the position and angle of the detector, and the anisotropic scattering of the media, are incorporated. The sensitivity and accuracy of the MC method are examined. The MC method is used to simulate a 60 ps laser pulse transport through a block containing scattering silica micro-spheres. The predicted temporal transmittance is compared with the experimental measurement. The influence of the refractive index of the scattering particles is discussed.

MONTE CARLO MODEL

The pulse laser source is normally incident upon the participating medium from the origin of the Cartesian coordinates. The incident laser intensity is axisymmetric and has temporal and spatial Gaussian profiles expressed by

$$I_c(x,y,z=0,t) = I_0 \exp\left[-4\ln 2 \times \left(\frac{t}{t_p} - 2\right)^2\right] \times \exp\left(-\frac{r^2}{\nu^2}\right) \tag{1}$$

where the pulse width, t_p, is full width at half maximum (FWHM), $r^2 = x^2 + y^2$, and $\nu^2/2$ is the spatial variance of the Gaussian incident beam. In the present study, the input pulse is simulated at the time range $t \subseteq [0, 4t_p]$ for Gaussian temporal profile.

The anisotropic scattering phase function is specified by the Henyey-Greenstein form as follows:

$$\Phi(\mu) = \frac{1-g^2}{(1+g^2-2g\mu)^{3/2}} \tag{2}$$

where, $\mu = \cos(\theta)$. Fresnel reflection is taken into account at the medium/air boundaries, where Snell's law is obeyed: $n_s \sin\theta_i = \sin\theta_r$. In which, the incident angle is θ_i, and refraction angle is θ_r. Since the refractive index of the medium $n_s > 1$, when $\theta_i \geq \sin^{-1}(1/n_s)$, total reflection occurs at the boundaries. When $\theta_i < \sin^{-1}(1/n_s)$, the reflectance between the random walk medium and air is given by the Fresnel equation as

$$\rho = \frac{1}{2}\left[\frac{\tan^2(\theta_i - \theta_r)}{\tan^2(\theta_i + \theta_r)} + \frac{\sin^2(\theta_i - \theta_r)}{\sin^2(\theta_i + \theta_r)}\right]. \tag{3}$$

The position (x, y, ψ) of the incidence of the laser photon bundles on the $z = 0$ interface is derived as:

$$r = \nu\sqrt{\ln\left[1 - R\left(1 - \exp(-r_i^2/\nu^2)\right)\right]^{-1}} \tag{4}$$

$$\psi = 2\pi R \tag{5}$$

$$x = r\cos\psi, \quad y = r\sin\psi \tag{6}$$

in which R is random number generated by the computer using random seed, and r_i is the beam radius.

The distance that any one bundle may travel before absorption or scattering is

$$D = [\ln(1/R)]/\beta\,. \tag{7}$$

The deposit fraction by absorption is $1-\omega$, where ω is scattering albedo. For the temporal analysis, the total optical path length of each ray inside the medium is converted to time of flight by using the speed of light in the medium

$$t = D/c = D \times n_s / c_0\,. \tag{8}$$

The direction of light propagation after scattering is determined by

$$\begin{cases} \psi' = 2\pi R \\ \theta' = \cos^{-1}\left\{\dfrac{1+g^2-[(1-g^2)/(1+g-2gR)]^2}{2g}\right\} \end{cases} \tag{9}$$

where the polar angle θ' is measured from an axis pointing in the incoming direction of the radiation and the circumferential angle ψ' is measured in a plane normal to the incoming direction.

Other details about the implement of transient Monte Carlo model and numerical procedure have been described in recent publications [12,17].

EXPERIMENT

The experimental setup is shown in Fig. 1. The apparatus is composed of three primary parts: a short pulse laser source unit, a sample cell, and an ultrafast detecting unit. Laser pulses of 60 ps at a repetition rate of 76 MHz were generated from frequency-doubled Nd^{+3}:YAG mode-locked laser. The beam diameter is 1.3 mm. A beamsplitter diverts 10% of the 532 nm, 60 ps, 76 MHz laser pulse train to a power meter to monitor the intensity of the incident pulse. The sample is mounted, stationary, in the center of a rotary stage, with an optical fiber mount attached to the rotary platen. The scattered light is collected by an approximately 100 micron optical fiber whose angular position relative to the incident laser beam's axis can be accurately varied by rotating the mount, enabling monitoring of the angular distribution, intensity and temporal profile of the scattered light by a Hamamatsu OOS-01 optical oscilloscope. The halfwave plate/polarizer combination controls both polarization and the incident power on the sample. An adjustable mask with a circular aperture placed on the output face of the sample limits the area whose scattered output is monitored.

The sample is a three-dimensional block and is made to model similar optical properties of artificial biological tissues. In the process of making sample, amorphous silica micro-spheres of very regular shape, diameter 1000nm +/- 10%, were dispersed in styrene, which was then polymerized. These cast solids, typically about 0.81% v/v loaded in the present study, have the advantage of flexibility of shape, minimal number of interfaces to account for in modeling, and lack of convective motion from localized heating due to absorption. Absorption is negligible in the polymer matrix for visible wavelengths, and can be adjusted by mixing dyes into the styrene before polymerization.

RESULTS AND DISCUSSION

At first, we examine the MC method in short pulse transport through a cube with a weakly absorbing and highly scattering medium. The side length of the cube is 10 mm. The medium properties are assumed to be n_s = 1.59, β = 10 mm^{-1}, ω = 0.998, and g = 0.9. The incident pulse properties are t_p = 60 ps, and r_i = 1.3 mm.

Figure 2 shows the temporal profiles of normalized transmittances from different azimuthal angles at the center of the cube output surface. Various transmitted azimuthal angles are selected from θ = 0 to 80 degree with increment = 10 degree. For comparison, hemispherical transmittance is also plotted. It is seen that the temporal shapes of the transmitted pulse at different azimuthal angles are very similar, so that a hemispherical transmittance could be used to represent the transmittance detected at specific angle. However, it should be noted that such a conclusion is only valid in the case of optically thick medium, which is usually encountered in bioengineering applications [2].

The MC result is a sample mean calculated from 30 independent runs in the above example. The statistical errors (standard deviation of the mean) and relative statistical errors (standard deviation over mean) in hemispherical transmittance are drawn in Fig. 3. Two different ray numbers are selected in each run for comparison, i.e., nray = 10^6, and 3×10^6, respectively. The profile of absolute statistical error follows the profile of the transmittance. In other words, the absolute statistical error is smaller when the corresponding transmittance is smaller. However, the trend of relative statistical error is reverse, i.e., the relative statistical error is smaller when the corresponding transmittance is larger. With the increase of the ray number in each run, the statistical errors become smaller. Theoretically, the statistical error could be driven to near zero, but this would increase dramatically the computation time. The computation time is linearly proportional to the value of ray number. It is seen that, the statistical errors in the case of nray = 3×10^6 are generally smaller than the case of nray = 10^6. However, the improvement of the accuracy converges slowly compared with the increase of computation time. Thus, there should be a compromise of trade-off between accuracy and computation cost. In the present study, we mainly focus on the prediction of the transmitted pulse shape. From Fig. 3, it is seen that the relative uncertainty in most range of the temporal shape is less than 5%.

Figure 4 shows the temporal profiles of relative transmittance for input pulse with various pulse widths. Other parameters are the same as aforementioned. The input pulses have Gaussian temporal profile as described in equation (1). The system radiation propagation time (= character length L / light speed c in the medium) for the cube is about 53 ps. The importance of transient effect in short pulse laser radiation transfer is clearly demonstrated when the input pulse width is smaller than the radiation propagation time in the medium, i.e., the output pulse width is significantly enlarged. In the case of input pulse width t_p = 1 ps, the transmitted pulse has a fast response at early time instants and then a long decaying tail. With the increase of input pulse width until the same order of the system propagation time, the transmitted pulse does not change perceptibly, except that the rising at the early time becomes slower. Even in the case of t_p = 100 ps, i.e., the input pulse width is about two times larger than the system propagation time, the broadening of the transmitted pulse is still obvious. However, when the input pulse width is significantly larger than the system propagation time, e.g., t_p = 500 ps, the broadening of the transmitted pulse is very slight and nearly invisible. Hence, a pseudo-steady state simulation without the consideration of light transient propagation effect is reasonable when the input pulse width is considerably larger than the system propagation time.

In Fig. 5, the experiment measurement is presented and compared with MC simulation. The thickness of the sample is 14.4 mm. Other two dimensions are 49 mm × 47.3 mm. Measurement

were performed at the azimuthal angles of 0, 30, 50, and 70 degree, respectively. The results are shown only for 0 and 30 degree detectors. The difference of normalized temporal transmittance between different angles is slight comparing with the measurement uncertainty. In experiment, we found that the uncertainty becomes larger with the increase of the detector azimuthal angle. This is because the magnitude of the transmitted intensity becomes smaller. We found that no matter at what angle the detector is, there exists a plateau in the temporal transmittance at the time period of 1000 ps < t < 1100 ps. At several trials, such a phenomenon did not disappear. It might be caused by the re-entry of backscattered pulse.

The bulk refractive index of the silica spheres is 1.458 at the wavelength of 589 nm [18], while a value of 1.417 was reported at the wavelength of 550 nm for individual silica beads by Firbank et al. [19]. When R.I = 1.417, the scattering coefficient and anisotropy of the sample are 17.052 mm^{-1} and 0.96276, respectively, predicted using the Mie theory. When R.I = 1.458, the scattering coefficient and anisotropy of the sample are 11.309 mm^{-1} and 0.96649, respectively. Thus, the prediction of the scattering properties of the sample is strongly influenced by the refractive index of the scattering particles. Such a difference also affects the MC simulation. In Fig. 5, it is seen that the predicted temporal profile of transmittance matches closely the experimental measurement in the case of R.I = 1.417. While in the case of R.I = 1.458, the MC predicted transmitted pulse width is obviously narrower than that of the experimental measurement. Since the volume load of silica micro-spheres in the present experiment is 0.81%, one should not use the bulk value of refractive index. Thus, R.I = 1.417 is the proper value for the individual silica micro-beads. The measurement of temporal transmittance might be a promising way for measuring refractive index of individual particles. The slight mismatch between prediction and measurement in the range of 500 < t <1000 ps can be explained by the different detector radii used in experiment and simulation. The detector in experiment is located 3 mm away from the output surface and its diameter is 100 μm. But the signal in the simulation is the hemispherical output from the mask attached at the surface and its radius is 750 μm. The research by Guo *et al.* [17] has revealed that the transmitted pulse width in larger radial position is wider. It is difficult to predict accurately the temporal behavior in a very small detector using forward MC method. A further work using backward MC method might be required.

The CPU time spent in the MC simulation of the above experiment in the purely scattering sample was about 108 hrs in a PC with one Pentium III Xeon 500 MHz processor. In order to reduce the computation cost, one might exploit the use of isotropic scattering scaling law, which scales the anisotropic scattering into an equivalent isotropic scattering. The isotropic scaling usually gives reasonable accuracy in steady state radiative transfer. In the MC simulation of scaled isotropic scattering, the CPU time is 2.23 hrs, which is only 2.1% of the CPU time used in anisotropic scattering modeling. However, the comparison of the results as shown in Fig. 6 illustrates that the scaled isotropic scattering cannot predict accurate temporal behavior of the transmittance. This is consistent with the one-dimensional study of Guo and Kumar [12], where it was found that the isotropic scaling is only suitable for optically very diffuse medium (after isotropic scaling) with forward scattering and at the long time stages. At the early time period, the isotropic scaling allows a large fraction of direct transmission without the interaction with the medium. However, such a ballistic transmission is not visible in the simulation using anisotropic scattering phase function because of the zig-zag behavior of multiple scattering events in photon transport. Thus, the modeling of anisotropic scattering is usually required in short pulse laser transport through scattering medium.

CONCLUSIONS

The Monte Carlo method is used to simulate the short pulse laser radiation transport through three-dimensional scattering-absorbing media. The simulation is compared with experimental measurement in scattering medium. It is found that, when the optical thickness of the medium is considerably large, the difference of temporal shapes between different azimuthal angles is slight. In other words, the temporal profile of the transmitted pulse is not a function of the output azimuthal angle. The experimental measurement also demonstrates that the temporal shapes of the transmitted pulse (except the magnitude of the amplitude) at various angles are very similar. This implies that it might be reasonable to simulate the transmitted pulse at specific detector angles using the hemispherical flux distribution. However, it should be pointed out that the uncertainty in the experiment is not small. The use of an accurate value of the refractive index of the scattering particles is very important in simulation. Even an error of several percent will change the scattering properties, and consequently change the prediction of the temporal behavior of pulse transfer. The use of scaled isotropic scattering will save dramatically computational cost, but the accuracy is not sufficient.

ACKNOWLEDGMENTS

The authors acknowledge partial support from the Sandia-NSF joint grant AW-9963 (CTS-973201) administered by Sandia National Lab, Albuquerque, Dr. Shawn P. Burns, Project Manager.

REFERENCES

1. Kumar, S. and Mitra, K., Microscale Aspects of Thermal Radiation Transport and Laser Applications, *Advances in Heat Transfer*, Vol. 33, pp.187-294, 1998.

2. Yamada, Y., Light-Tissue Interaction and Optical Imaging in Biomedicine, *Annual Review of Heat Transfer*, Vol. 6, pp. 1-59, 1995.

3. Mitra, K. and Churnside, J. H., Transient Radiative Transfer Equation Applied to Ocenographic Lidar, Appl. Opt., Vol. 33, pp. 889-895, 1999.

4. Longtin, J. P. and Tien, C. L., Microscale Radiation Phenomena, *Miscroscale Energy Transfer*, Taylor and Francis, Washington, D. C., pp. 119- 147, 1997.

5. Madsen, S. J., Wilson, B. C., Patterson, M. S., Park, Y. D., Jacques, S. J., and Hefetz, Y., Experimental Tests of a Simple Diffusion Model for the Estimation of Scattering and Absorption Coefficients of Turbid Media from Time-Resolved Diffusion Reflectance Measurements, *Appl. Opt*., Vol. 31, pp. 3509-3517, 1992.

6. MacKintosh, F. C., Zhu, J. X., Pine, D. J. and Weitz, D.A., Polarization Memory of Multiply Scattered Light, Phys. Rev. B, Vol. 40, pp. 9342 – 9345, 1989.

7. Yoo, K. M., Liu, F., and Alfano, R. R., When Does the Diffusion Approximation Fail to Describe Photon Transport in Random Media, *Phys. Rev. Lett.*, Vol. 64, pp. 2647-2650, 1990.

8. Kumar, S., and Mitra, K., Transient Radiative Transfer, *Radiative Transfer* – I, Begell House, New York, pp. 488-504, 1995.

9. Kumar, S., Mitra, K., and Yamada, Y., Hyperbolic Damped-Wave Models for Transient Light-Pulse Propagation in Scattering Media, *Appl. Opt.*, Vol. 35, pp. 3372-3378, 1996.

10. Rackmil, C. I., and Buckies, R. O., Numerical Solution Technique for the Transient Equation of Transfer, *Numerical Heat Transfer*, Vol. 6, pp. 135-153, 1983.

11. Mitra, K., Lai, M.-S., and Kumar, S., Transient Radiation Transport in Participating Media Within a Rectangular Enclosure, *J. Thermophy. Heat Transfer*, Vol. 11, pp. 409-414, 1997.

12. Guo, Z. and Kumar, S., Equivalent Isotropic Scattering Formulation for Transient Short-Pulse Radiative Transfer in Anisotropic Scattering Planar Media, Appl. Opt., Vol. 39, pp. 4411-4417, 2000.

13. Tan, Z. M. and Hsu, P.-F., *Proc. of 34th National Heat Transfer Conference*, NHTC2000-12077, Pittsburgh, August 20-22, 2000.

14. Siegel, R., and Howell, J. R., *Thermal Radiation Heat Transfer* (3rd ed.), Hemisphere, Washington, 1992.

15. Flock, S. T., Patterson, M. S., Wilson, B. C., and Wyman, D. R., Monte Carlo Modelling of Light Propagation in Highly Scattering Tissues-I: Model Predictions and Comparison with Diffusion Theory, *IEEE Trans. Biomedical Engr.*, Vol. 36, pp. 1162-1167, 1989.

16. Hasegwa, Y., Yamada, Y., Tamura, M. and Nomura, Y., Monte Carlo Simulation of Light Transmission Through Living Tissues, *Appl. Opt*., Vol. 30, pp. 4515-4520, 1991.

17. Guo, Z., Kumar, S. and San, K.-C., Multidimensional Monte Carlo Simulation of Short-Pulse Laser Transport in Scattering Media, *J. Thermophy. Heat Transf*., Vol. 14, pp. 504-511, 2000.

18. Mark, J. E., ed., *Physical Properties of Polymers Handbook*, AIP Press, Woodbury, NY 1996.

19. Firbank, M., Oda, M., and Delpy, D.T., An Improved Design for a Stable and Reproducible Phantom Material for Use in Near-Infrared Spectroscopy and Imaging, *Phys. Med. Biol*., Vol. 40, pp. 955-961, 1995.

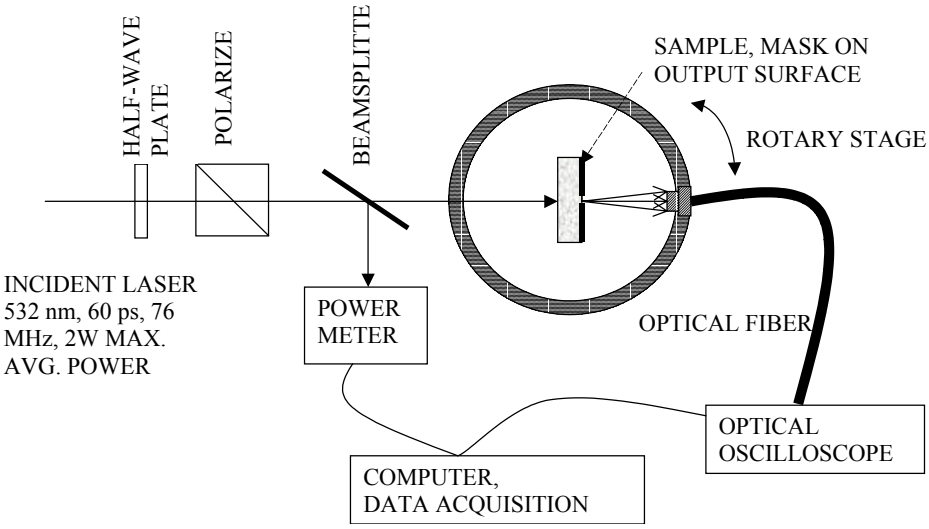

Figure 1. Experimental setup.

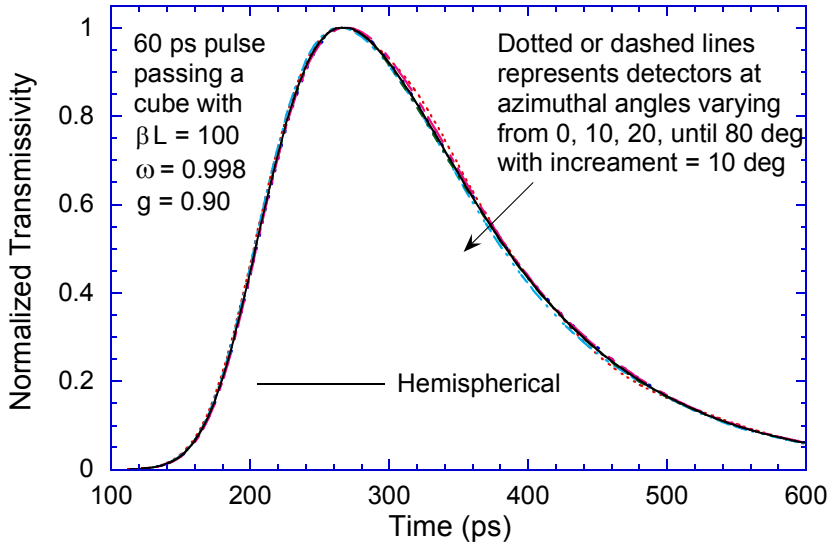

Figure 2. Temporal profiles of normalized transmittance detected at various output angles.

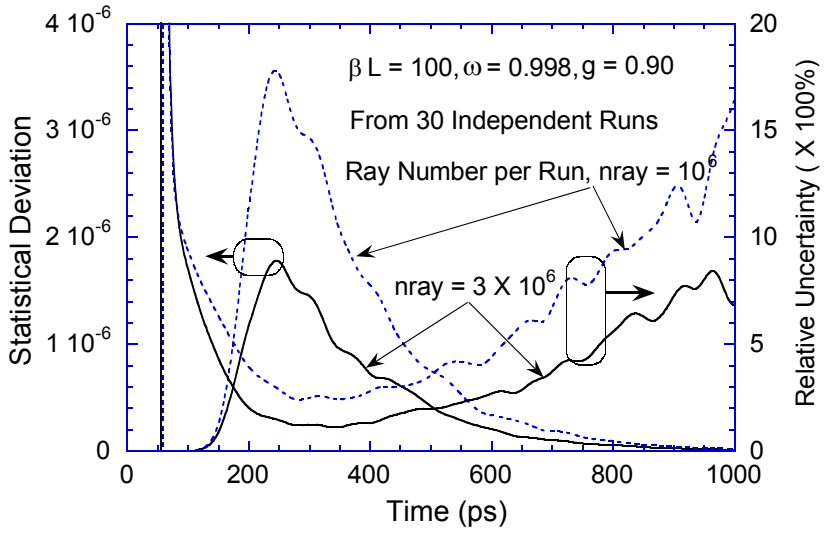

Figure 3. Numerical uncertainty of the mean hemispherical transmittance.

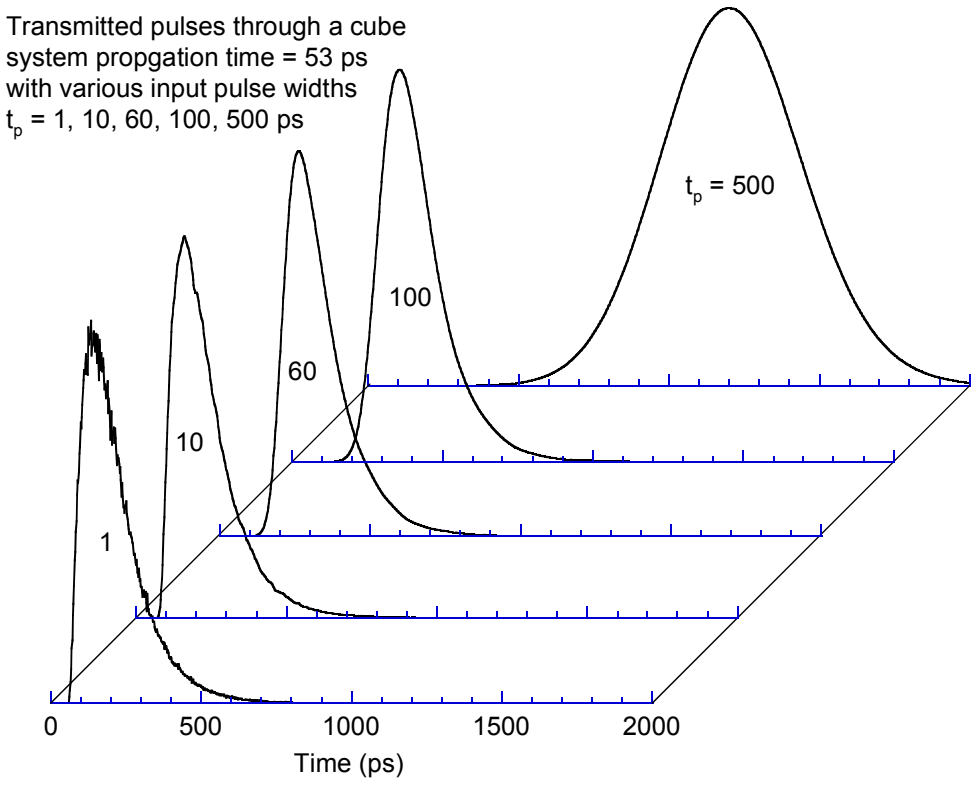

Figure 4.The broadening of transmitted pulse with different input pulse widths.

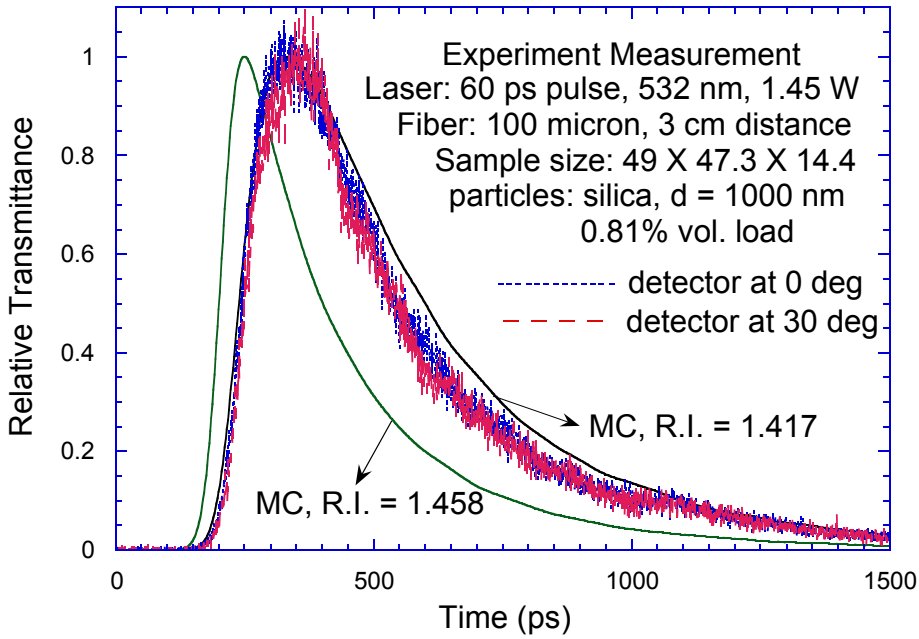

Figure 5. Experimental measurements and comparison with MC simulations for a 60 ps laser pulse passing through a purely scattering medium.

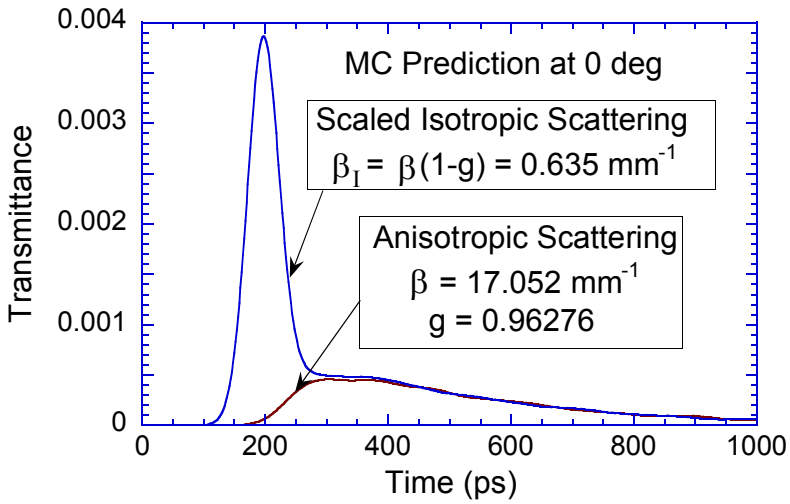

Figure 6. Comparison of temporal profiles of transmittance between predictions of anisotropic scattering model and scaled isotropic scattering model.